Impact of a Permo-Carboniferous high O_2 event on the terrestrial carbon cycle

D. J. Beerling*† and R. A. Berner‡

*Department of Animal and Plant Sciences, University of Sheffield, Sheffield S10 2TN, United Kingdom; and ‡Department of Geology and Geophysics, Yale University, New Haven, CT 06520-8109

Edited by Steven M. Stanley, Johns Hopkins University, Baltimore, MD, and approved September 5, 2000 (received for review June 17, 2000)

Independent models predicting the Phanerozoic (past 600 million years) history of atmospheric O_2 partial pressure (pO_2) indicate a marked rise to approximately 35% in the Permo-Carboniferous, around 300 million years before present, with the strong potential for altering the biogeochemical cycling of carbon by terrestrial ecosystems. This potential, however, would have been modified by the prevailing atmospheric pCO_2 value. Herein, we use a process-based terrestrial carbon cycle model forced with a late Carboniferous paleoclimate simulation to evaluate the effects of a rise from 21 to 35% pO_2 on terrestrial biosphere productivity and assess how this response is modified by current uncertainties in the prevailing pCO_2 value. Our results indicate that a rise in pO_2 from 21 to 35% during the Carboniferous reduced global terrestrial primary productivity by 20% and led to a 216-Gt (1 Gt = 10^{12} kg) C reduction in the vegetation and soil carbon storage, in an atmosphere with pCO_2 = 0.03%. However, in an atmosphere with pCO_2 = 0.06%, the CO_2 fertilization effect is larger than the cost of photorespiration, and ecosystem productivity increases leading to the net sequestration of 117 Gt C into the vegetation and soil carbon reservoirs. In both cases, the effects result from the strong interaction between pO_2, pCO_2, and climate in the tropics. From this analysis, we deduce that a Permo-Carboniferous rise in pO_2 was unlikely to have exerted catastrophic effects on ecosystem productivity (with pCO_2 = 0.03%), and if pCO_2 levels at this time were >0.04%, the water-use efficiency of land plants may even have improved.

Atmospheric O_2 is a key gas regulating the metabolism of the Earth's aerobic biota. A Phanerozoic (past 600 million years) history of atmospheric O_2 partial pressure (pO_2) shows that pO_2 over much of this time was relatively stable as a result of a variety of geological and biological feedbacks, with an important excursion to about 35% centered at around 300 million years B.P. during the Permo-Carboniferous (see ref. 1 by Berner for a review). This marked pO_2 increase results from the evolution of vascular land plants on the continents (2, 3) and enhanced burial of recalcitrant organic matter in swamps (4), the latter being represented by abundant and widespread coal deposits of this age. The high Permo-Carboniferous value was calculated originally from the abundance of organic carbon and pyrite sulfur (FeS_2) in sedimentary rocks, because global fluxes of reduced carbon and sulfur are the two dominant pO_2 controls on a time scale of millions of years (1–3). More recently, an independent approach to modeling Phanerozoic pO_2 evolutionary history, by using global carbon and sulfur isotope mass balance analyses and incorporating O_2-sensitive isotope fractionation by the terrestrial and marine biota (5), closely reproduced the large pO_2 peak at 300 million years B.P.; this excursion is consistent with biological data from the fossil record such as the sudden rise and fall in insect gigantism (6).

Given that two rather different approaches to modeling pO_2 history in the atmosphere point to a high Permo-Carboniferous pO_2 value, there is a need to assess its likely effects on the photosynthetic productivity of vascular land plants and the terrestrial biosphere as a whole at this time. The need is underscored, because the dual carboxylase-oxygenase function of Rubisco (ribulose-1,5-bisphosphate carboxylase/oxygenase), the primary CO_2-fixing enzyme of C_3 land plants, is influenced strongly by atmospheric pO_2 and pCO_2, with the potential to modify the biogeochemical cycling of carbon by terrestrial ecosystems. Carboxylation leads to photosynthesis via the photosynthetic carbon reduction pathway, and oxygenation leads to photorespiration via the carbon oxidation pathway, with the evolution of CO_2 (7). A high pO_2 atmosphere favors the oxygenation reaction of Rubisco, with O_2 tending to out compete CO_2 for the acceptor molecule ribulose bisphosphate, leading to increased photorespiration and decreased net photosynthetic CO_2 fixation (7). However, crucial to determining the oxygenation/carboxylation ratio of Rubisco is the prevailing pCO_2 value, and for the Permo-Carboniferous, some uncertainty exists regarding its value. Estimates of pCO_2 during the late Carboniferous from soil carbonates and organic matter (8) overlap those made from theoretical considerations of the long-term carbon cycle (9); however, these estimates encompass a range of values (between 0.03 and 0.08%). A simple consideration of Rubisco kinetics leads to the expectation that this range will be critical for determining the impact of 35% O_2 on rates of photosynthetic CO_2 uptake (10–12).

Temperature further exerts an important modifying influence on the efficiency of Rubisco, by altering the relative solubility of CO_2 and O_2 and the specificity of Rubisco for CO_2 (11, 12). Consequently, pCO_2, O_2, and climate will all interact to modify carbon cycling by terrestrial ecosystems, and such interactions require a global-scale approach for an adequate assessment of the Permo-Carboniferous high O_2 event on the biosphere. Herein, we take the global view to assess first the effect of a rise in pO_2 from 21 to 35% on the primary productivity of terrestrial vegetation and carbon storage in vegetation biomass and soil organic matter at a constant pCO_2 content (0.03%) by using a process-based terrestrial carbon cycle model (13, 14) forced with a global general circulation model (GCM) simulation of the late Carboniferous climate (15, 16). We next determine through a series of sensitivity experiments how this response is modified by uncertainties in the Permo-Carboniferous pCO_2. Changes in the possible functioning of the terrestrial biosphere at this time, as predicted by the model, are compared and discussed with data from plant growth experiments in which the pO_2 and pCO_2 values were manipulated.

Materials and Methods

Terrestrial Carbon Cycle Modeling. The University of Sheffield terrestrial carbon cycle model simulates, under steady-state

This paper was submitted directly (Track II) to the PNAS office.

Abbreviations: pO_2, O_2 partial pressure; pCO_2, CO_2 partial pressure; Rubisco, ribulose-1,5-bisphosphate carboxylase/oxygenase; GCM, general circulation model; NPP, net primary productivity.

†To whom reprint requests should be addressed. E-mail: d.j.beerling@sheffield.ac.uk.

The publication costs of this article were defrayed in part by page charge payment. This article must therefore be hereby marked "*advertisement*" in accordance with 18 U.S.C. §1734 solely to indicate this fact.

Article published online before print: *Proc. Natl. Acad. Sci. USA*, 10.1073/pnas.220280097. Article and publication date are at www.pnas.org/cgi/doi/10.1073/pnas.220280097

Table 1. Global terrestrial NPP and carbon storage in vegetation biomass and soil carbon reservoirs during the late Carboniferous

Simulation	NPP, Gt C yr^{-1}	Vegetation biomass, Gt C	Soil organic matter, Gt C
Case 1. 21% O_2, 0.03% CO_2 (control case)	47	473	1,004
Case 2. 35% O_2, 0.03% CO_2	38 (−9)	373 (−100)	888 (−116)
Case 3. 35% O_2, 0.045% CO_2	44 (−3)	463 (−10)	984 (−20)
Case 4. 35% O_2, 0.06% CO_2	50 (+3)	554 (+81)	1,084 (+80)

Results were obtained by forcing the terrestrial carbon cycle with the same climate with different prescribed pO_2 and pCO_2 values. Values in parentheses denote the differences relative to the control case. Note that 1 Gt = 10^{12} kg.

conditions of climate and atmospheric composition (CO_2 and O_2), the basic plant processes of photosynthesis, respiration, and transpiration (13, 14). Canopy transpiration is regulated by stomatal conductance and feeds back to influence soil water status. The aboveground productivity module is dynamically coupled to the Century biogeochemistry model (17) describing the cycling of carbon and nitrogen in soils. Surface litter inputs (leaves and roots) derived from the vegetation are decomposed through the various Century routines to compute soil nutrient status that, in turn, influences vegetation primary productivity. Equilibrium model solutions were obtained by iteration under a given climate and atmospheric composition for 500 years. The key model outputs are net primary productivity (NPP), leaf area index, canopy transpiration, and carbon storage in vegetation biomass and soil organic matter.

Paleoclimate Simulations. In all of the modeling experiments described herein, the carbon cycle model was forced with a global paleoclimate simulation (monthly temperature, precipitation, and relative humidity) representing the late Carboniferous, which was made by using the U.K. Universities' Global Atmospheric Modeling Program (UGAMP) GCM at the University of Reading (Reading, U.K.). A full description of this model is given by Valdes *et al.* (18). Briefly, the model has a horizontal spatial resolution of 3.75° × 3.75° with 19 levels in the vertical. Continental positions were similar to those used by Crowley and Baum (19); other major boundary conditions were 3% lower solar luminosity than the present day, a pCO_2 value of 300 ppm, and orbital configuration of the Pleistocene interglacials. The simulation used prescribed sea surface temperatures based on energy balance results that were energetically consistent with the choice of CO_2 and solar constant. The model was integrated for 5 years, and data from the last 2 years were averaged to produce the Carboniferous climate. Further details of the simulation and resulting global patterns of mean annual temperature and precipitation are given by Beerling *et al.* (15) and Valdes and Crowley (16).

Model Experiments. To assess the effect of the Permo-Carboniferous rise in O_2 and the uncertainty in pCO_2 on the terrestrial carbon cycle, four simulations were performed. The first, at 21% O_2 and 0.03% CO_2, defines case 1, the "control." Three simulations were then made at 35% O_2, each with a different pCO_2 level (0.03%, case 2; 0.045%, case 3; 0.06%, case 4); these three pCO_2 values represent, respectively, lower, "best guess," and upper estimates from theoretical modeling (20). A Permo-Carboniferous pO_2 value of 35% was taken from two geochemical model predictions (3, 5). Each pCO_2 and pO_2 value was prescribed within the aboveground vegetation productivity module of the terrestrial carbon model. In that module, CO_2 and O_2 act on rates of photosynthesis through the well validated, biochemically based mechanistic model of leaf photosynthesis of Farquhar *et al.* (21). All simulations were performed with the same GCM paleoclimate data set for different prescribed pCO_2 and pO_2 values. We assume that plants with the C_3 photosynthetic pathway dominated Carboniferous floras, because there is only limited and equivocal evidence for plants operating with any other photosynthetic pathway in the Carboniferous (e.g., ref. 22).

Results and Discussion

We first assessed the effect of a marked Permo-Carboniferous rise in pO_2 on global terrestrial biosphere productivity under the late Carboniferous GCM paleoclimate, assuming a constant 0.03% pCO_2 value. Comparison of the two appropriate simulations (cases 1 and 2) indicate a rise from 21 to 35% O_2 reduced global vegetation productivity by 20% (Table 1 and Fig. 1). Under these circumstances, this reduction implies high O_2 impacts on the oxygenation/carboxylation reactions of Rubisco within individual leaves, which influence the operation of the terrestrial biosphere, even under the relatively cool Carboniferous paleoclimate. However, sensitivity analyses indicate that if the same rise in pO_2 occurred in an atmosphere with pCO_2 = 0.06% (case 4), then the CO_2 fertilization effect on photosynthetic productivity is larger than the cost of photorespiration, such that terrestrial NPP actually increases by 3 Gt C per yr^{-1} (Table 1). The intermediate case 3, with pCO_2 = 0.045%, results in the inhibitory effects of high O_2 on vegetation productivity being largely cancelled out (Table 1). In this scenario, therefore, severe suppression of terrestrial productivity by plants with the C_3 photosynthetic pathway and their interactions with resource availability owing to a Permo-Carboniferous pO_2 excursion would seem unlikely.

Plant growth experiments with different pO_2/CO_2 values support the direction of change in NPP revealed by these model simulations. For example, a 20% reduction in global NPP through a rise in pO_2 to 35% is mirrored by an observed 30% reduction in the photosynthetic rates of *Betula pubescens* leaves when measured at 21 and 35% pO_2 (15). At the whole plant scale, changes in leaf photosynthesis translate to lowered plant biomass (10, 23, 24) with the vegetative biomass of *Pancium bisulcatum* being reduced by 30% after 24 days of growth in 40% O_2 compared with 21% (24). The compensatory effects of increasing pCO_2 during a high pO_2 event, as indicated by the model results (Table 1 and Fig. 1), is also supported by growth experiments (23, 25). The growth of soybean (*Glycine max*) was reduced from 28 g per plant (dry mass) at 21% O_2 and 0.03% CO_2 to 15 g per plant when the pO_2 value was increased to 40% (23); however, as with the terrestrial biosphere response, this effect was strongly diminished when plant growth pCO_2 was increased to 0.07%.

Annual changes in NPP caused by a Permo-Carboniferous pO_2 rise feed through to influence the resulting size of the carbon reservoirs in vegetation biomass and soils in a manner that mirrors the NPP responses (Table 1). When the pO_2 rise occurred with pCO_2 = 0.03%, shown by the difference between case 1 and 2, reductions in NPP occurred throughout

GEOLOGY

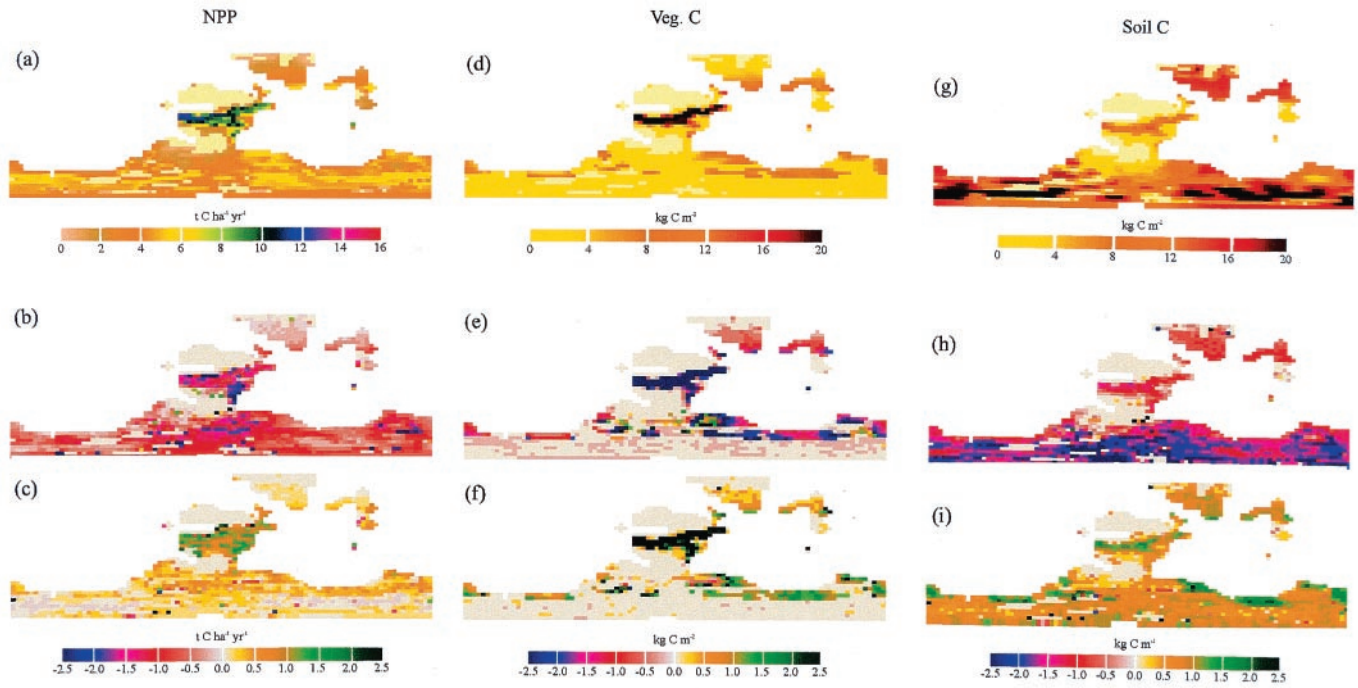

Fig. 1. Global distribution of NPP (t C per $ha^{-1}\cdot yr^{-1}$), vegetation biomass (kg C per m^{-2}), and soil carbon concentrations (kg C per m^{-2}) in the late Carboniferous for the atmospheric composition represented by the control case (21% O_2, 0.03% CO_2; *a*, *d*, and *g*, respectively), and the modeled effects of the Permo-Carboniferous pO_2 increase at two different pCO_2 levels, given as the difference between case 2 (35% O_2, 0.03% CO_2) and the control (*b*, *e*, and *h*) and between case 4 (35% O_2, 0.06% CO_2) and the control (*c*, *f*, and *i*). Note that maps *b*, *c*, and *h* as well as *c*, *f*, and *i* are difference maps and are plotted on different scales. Each individual map shows the three major landmasses of the land-sea mask used in the climate and vegetation modeling. These were Gondwana, dominating the Southern hemisphere; Eurasia, the largest Northern hemisphere landmass; and adjacent to this landmass, Kazakhstan.

each of the major landmasses (Fig. 1*b*). However, the geographical extent of reductions in the vegetation carbon pool is more localized than that of NPP, being restricted to the northern margins and throughout central Gondwana (Fig. 1*e*). This result reflects the loss of accumulated carbon from forests (26). Similarly, it is only in these same forested regions where vegetation biomass increases when the pO_2 rise is simulated together with an associated rise in pCO_2 to 0.06% (Fig. 1*f*), because these are the only dominant plant functional types able to store significant additional carbon in stem biomass gained from increased NPP.

The response of the soil carbon pool to the prescribed pO_2 and pCO_2 values is geographically more widespread than the response of vegetation biomass (Fig. 1), because the soil surface carbon pool has a faster turnover time (27) and is therefore quite responsive to O_2-induced changes in litter production. In consequence, the pattern and direction of change in the size of the soil carbon reservoir is similar to that of NPP (Fig. 1). A rise in pO_2 to 35% with pCO_2 = 0.03% (case 2), for example, reduces soil carbon concentrations (relative to the control, case 1; Fig. 1*h*); this rise occurs, because the soils receive reduced surface litter input (leaves and roots) from the vegetation but, under the given GCM climate, are subjected to the same proportion of CO_2 being lost through plant and soil respiration. A rise in pO_2 with pCO_2 = 0.06% (the difference between cases 4 and 1) increases the soil carbon reservoir (Fig. 1*i*) reflecting higher production rates of surface litter organic matter by the vegetation and a high C:N ratio caused by plant growth in a high pCO_2 environment. Globally, the total differences in the vegetation carbon reservoir resulting from a rise in pO_2 with various pCO_2 values were similar to those in the soil carbon reservoir (Table 1).

The global-scale terrestrial carbon cycle simulations allow us to asses how climate modifies the pCO_2 and pO_2 interactions on Rubisco efficiency and, in turn, how this modification influences annual NPP. These interactions are brought out clearly by the latitudinally averaged NPP responses for each case, when expressed relative to the control (case 1; Fig. 2). This plot indicates that the largest modification of the high O_2 response by different pCO_2 values occurs in the warm equatorial regions. In case 2 (pO_2 = 35% and pCO_2 = 0.03%), the oxygenation reaction dominates, leading to increased photorespiratory CO_2 losses and a net reduction in NPP (Fig. 2). However, when the O_2 rise is simulated with pCO_2 = 0.06% (case 4), the carboxylation

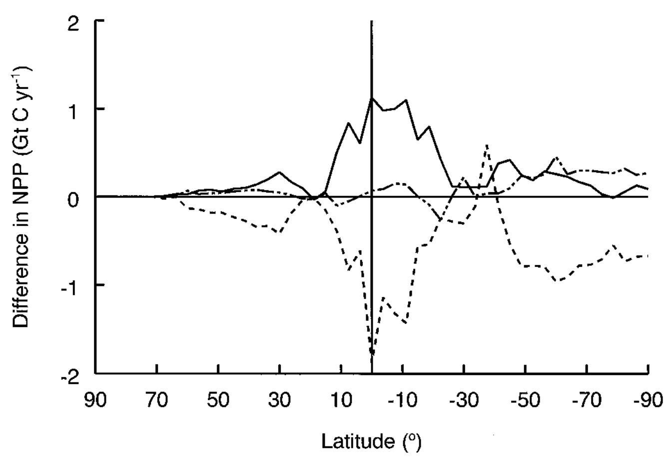

Fig. 2. Effects of the Permo-Carboniferous pO_2 rise at three different pCO_2 levels on the latitudinal gradient of terrestrial NPP during the late Carboniferous. The gradients represent the difference between the case 2 and the control simulation (21% O_2, 0.03% CO_2; dashed line), case 3 and the control simulation (dot-dash line), and case 4 and the control simulation (solid line).

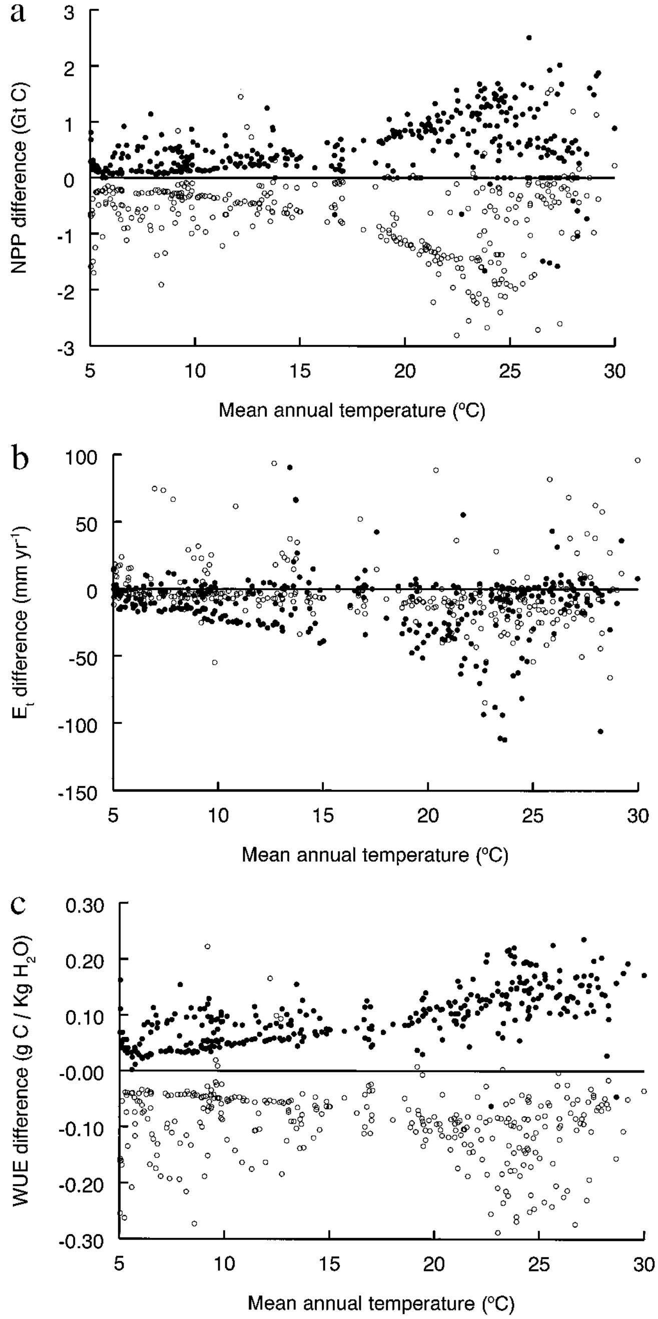

Fig. 3. Effects of the Permo-Carboniferous pO_2 rise at two different pCO_2 levels on annual (*a*) terrestrial NPP, (*b*) canopy transpiration (E_t), and (*c*) water-use efficiency (WUE, defined as NPP divided by E_t) during the late Carboniferous, analyzed on a site-by-site basis. Open symbols represent results from case 2 (35% O_2, 0.03% CO_2); solid symbols represent results from case 4 (35% O_2, 0.06% CO_2). All values are expressed as the differences between results from the specified atmospheric composition and the control (case 1).

reaction of Rubisco dominates, allowing NPP to increase in those regions, whereas the intermediate case (Table 1) shows that the effects of a Permo-Carboniferous pO_2 of 35% are largely cancelled by an atmosphere with $pCO_2 = 0.045\%$ (Fig. 2).

Analysis on a site-by-site basis (i.e., individual grid squares) for cases 2 and 4 clearly separates these divergent climate interactions on Rubisco, where the mean annual temperature is >5°C (Fig. 3*a*). Vegetation operating in an atmosphere defined by case 2 ($pO_2 = 35\%$, $pCO_2 = 0.03\%$) shows a progressive reduction with temperature in NPP relative to the control at sites where the mean annual temperature is between 5 and 30°C (Fig. 3), because increasing temperature favors the oxygenation of ribulose bisphosphate by decreasing, relative to O_2, both the solubility of CO_2 and specificity of Rubisco for CO_2 (11, 12). Between temperatures of 7 and 35°C, the specificity effect accounts for two-thirds of the reduction in NPP, and the solubility effect accounts for the remaining third (12). In a high CO_2 environment, the opposite effect occurs, with NPP increasing as the mean annual temperature rises, despite the high pO_2 value (Fig. 3*a*), because the key effect of elevated pCO_2 is increased competitive inhibition of oxygenation and hence photorespiration. The strong temperature-dependent oxygenation therefore is suppressed, and net photosynthetic rates rise proportionally. Such an effect is similar to that observed in gas exchange measurements on C_3 plants species under different pO_2 and pCO_2 conditions (28).

A consequence of lower photosynthetic rates in a high O_2 environment is that pCO_2 within the leaf rises, leading to partial stomatal closure (29–31), although this effect is not always the case at pO_2 values <35% (e.g., ref. 32). Such considerations lead to the suggestion that high O_2-induced shifts in stomatal conductance might alter canopy transpiration rates which, together with changes in photosynthetic productivity documented above, may have influenced vegetation water-use efficiency during the Permo-Carboniferous. To examine this suggestion, we first tested for the potential of leaf-scale stomatal pO_2 effects to upscale to whole canopies by comparing, on a site-by-site basis, canopy transpiration rates for cases 2 and 4 relative to the control. As intimated by leaf gas exchange measurements (29–31), the model data show that, at the majority of sites, annual canopy transpiration (E_t) was reduced relative to the control by a rise in pO_2 to 35% (Fig. 3*b*). For case 2 ($pO_2 = 35\%$, $pCO_2 = 0.03\%$), the reduction is brought about through lowered photosynthetic productivity reducing canopy conductance to water vapor and to a lesser extent leaf area index. For case 4, there is an overriding effect of $pCO_2 = 0.06\%$ that strongly reduces stomatal conductance, despite a small increase in leaf area index, and this reduction results in a much stronger decline in E_t (Fig. 3*b*). Combining the NPP and E_t responses for the two cases reveals a clear, previously unrealized difference in the response of vegetation water-use efficiency (Fig. 3*c*), suggesting that an elevated pO_2 episode during the Permo-Carboniferous could have influenced the water economy of vegetation.

Our results and those from growth experiments (10, 23–25) indicate that a Permo-Carboniferous high O_2 event, sustained for several million years with $pCO_2 \approx 0.03\%$, could have exerted strong selection pressures on the functioning of Rubisco, through favoring the oxygenation over carboxylation reaction. In this respect, it is intriguing to note that the timing of the pO_2 excursion predicted from geochemical models is similar to the date obtained from molecular clocks for the split between conifer-cycad and angiosperm lineages (33). In fact, the latter group of plants have stomatal characteristics that tend to maximize CO_2 diffusion into the leaf (34), thereby raising intercellular CO_2 concentrations and reducing CO_2 evolution by photorespiration (15). The timing and functional significance issues therefore suggest that a Permo-Carboniferous high O_2 episode might have triggered this split between major plant groups. Regardless, patterns of plant evolution seem to be at least circumstantially linked with the predictions of current models of Phanerozoic atmospheric O_2 history.

D.J.B. gratefully acknowledges funding through a Royal Society University Research Fellowship. R.A.B.'s research is supported by National Science Foundation Grant EAR 9417325 and Department of Energy Grant FG02–95ER14522.

1. Berner, R. A. (1999) *Proc. Natl. Acad. Sci. USA* **96,** 10955–10957.
2. Holland, H. D. (1978) *The Chemistry of the Atmosphere and Oceans* (Wiley, New York).
3. Berner, R. A. & Canfield, D. E. (1989) *Am. J. Sci.* **289,** 333–361.
4. Robinson, J. M. (1989) *Palaeogeogr. Palaeoclimatol. Palaeoecol.* **75,** 223–240.
5. Berner, R. A., Petsch, S. T., Lake, J. A., Beerling, D. J., Popp, B. N., Lane, R. S., Laws, E. A., Westerley, M. B., Cassar, N., Woodward, F. I., *et al*. (2000) *Science* **287,** 1630–1633.
6. Graham, J. B., Dudley, R., Aguilar, N. M. & Gans, C. (1995) *Nature (London)* **375,** 117–120.
7. Lawlor, D. W. (1993) *Photosynthesis: Molecular, Physiological and Environmental Processes* (Longman, Harlow, Essex, U.K.).
8. Mora, C. I., Driese, S. G. & Colarusso, L. A. (1996) *Science* **271,** 1105–1107.
9. Berner, R. A. (1998) *Philos. Trans. R. Soc. London B* **353,** 75–82.
10. Raven, J. A., Johnston, A. M., Parsons, R. & Kubler, J. (1994) *Biol. Rev.* **69,** 61–94.
11. Jordan, D. B. & Orgen, W. L. (1984) *Planta* **161,** 308–313.
12. Long, S. P. (1991) *Plant Cell Environ.* **14,** 729–739.
13. Woodward, F. I., Smith, T. M. & Emanuel, W. R. (1995) *Global Biogeochem. Cycles* **9,** 471–490.
14. Beerling, D. J. (2000) *Geophys. Res. Lett.* **27,** 253–256.
15. Beerling, D. J., Woodward, F. I., Lomas, M. R., Wills, M. A., Quick, W. P. & Valdes, P. J. (1998) *Philos. Trans. R. Soc. London B* **353,** 131–140.
16. Valdes, P. J. & Crowley, T. J. (1998) *Palaeoclim. Data Model.* **2,** 219–238.
17. Parton, W., Scurlock, J., Ojima, D., Gilmanov, T., Scholes, R., Schimel, D., Kirchner, T., Menaut, J. C., Seastedt, T., Moya, D., *et al*. (1993) *Global Biogeochem. Cycles* **7,** 785–809.
18. Valdes, P. J., Sellwood, B. W. & Price, G. D. (1996) *Palaeoclim. Data Model.* **2,** 139–158.
19. Crowley, T. J. & Baum, S. K. (1994) *Palaeoclim. Data Model.* **1,** 159–177.
20. Berner, R. A. & Kothavala, Z. (2001) *Am. J. Sci.*, in press.
21. Farquhar, G. D., von Caemmerer, S. & Berry, J. A. (1980) *Planta* **149,** 78–90.
22. Jones, T. P. (1994) *Rev. Palaeobot. Palynol.* **81,** 53–64.
23. Quebedeaux, B. & Hardy, R. W. F. (1975) *Plant Physiol.* **55,** 102–107.
24. Quebedeaux, B. & Chollet, R. (1977) *Plant Physiol.* **59,** 42–44.
25. Tolbert, N. E., Benker, C. & Beck, E. (1995) *Proc. Natl. Acad. Sci. USA* **92,** 11230–11233.
26. DiMichele, W. A. & Hook, R. W. (1992) in *Terrestrial Ecosystems Through Time: Evolutionary Paleoecology of Terrestrial Plants and Animals Through Time*, eds. Behrensmeyer, A. K., Damuth, D., DiMichele, W. A., Potts, R., Sues, H. D. & Wing, S. L. (Chicago Univ. Press, Chicago), pp. 205–325.
27. Trumbore, S. E. (1997) *Proc. Natl. Acad. Sci. USA* **94,** 8284–8291.
28. Sage, R. F. & Sharkey, T. D. (1987) *Planta* **84,** 658–664.
29. Gauhl, E. & Bjorkman, O. (1969) *Planta* **88,** 187–191.
30. Gale, J. & Tako, T. (1976) *Photosynthetica* **10,** 89–92.
31. Mikulska, M. & Maleszewski, S. (1990) *Photosynthetica* **24,** 607–612.
32. Rachmilevitch, S., Reuveni, J., Pearcy, R. W. & Gale, J. (1999) *J. Exp. Bot.* **50,** 869–872.
33. Savard, L., Li, P., Strauss, S. H., Chase, M. W., Michaud, M. & Bousuett, J. (1994) *Proc. Natl. Acad. Sci. USA* **91,** 5163–5167.
34. Beerling, D. J. (1994) *Philos. Trans. R. Soc. London B* **346,** 421–432.